UNIVERSIDAD COMPLUTENSE DE MADRID

PHYSICAL SCIENCE SCHOOL

Master in biomedical physics

MASTER DISSERTATION

RADIOCHROMIC FILM DOSIMETRY FOR MONITORING PRECLINICAL FLASH PROTONTHERAPY EXPERIMENTS

Irene Sanz García

Director

Daniel Sánchez Parcerisa

Academic course 2019/2020

INDEX

1. ABSTRACT

En este trabajo se ha realizado un estudio de la radioterapia FLASH tanto de forma teórica como de manera experimental. En primer lugar, el trabajo se centra en un estudio bibliográfico del estado del arte de la radioterapia FLASH. En segundo lugar, particularizando para protonterapia FLASH, se ha llevado a cabo la dosimetría de un experimento preclínico realizado por el Grupo de Física Nuclear (GFN) de la Universidad Complutense de Madrid (UCM). En este experimento distintas muestras fueron expuestas a protones de 3 MeV mediante irradiación FLASH y convencional. La dosimetría de dicho experimento, realizada en este trabajo, se lleva a cabo empleando películas radiocrómicas. En el proceso de dosimetría se ha realizado una calibración de las películas radiocrómicas que permite la posterior obtención de la dosis impartida a las distintas muestras del experimento. Además, las radiocrómicas también se han empleado para realizar medidas del perfil del haz. A su vez, se ha llevado a cabo un estudio teórico de la respuesta de las radiocrómicas en función del LET (transferencia lineal de energía) de los protones, concluyendo que estas realizan una subestimación de la dosis en las proximidades del pico de Bragg debido al efecto de *quenching*, Este estudio teórico se ha comprobado mediante los resultados experimentales obtenidos de las medidas de perfiles del haz y una simulación de Monte Carlo realizada con TOPAS.

In this work FLASH radiotherapy has been studied in a theoretical and experimental way. First, this work is based on a bibliographic research of the current state of the art. Secondly, the study is particularized on FLASH protontherapy. In this second part of the work, I conducted the dosimetry of a preclinical experiment made by the Group of Nuclear Physics (GFN) of Universidad Complutense de Madrid (UCM). In this experiment different samples were exposed to 3-MeV protons delivered with FLASH and conventional irradiation rates. The dosimetry of the experiment was performed with radiochromic (RC) films. This process required a prior calibration of the RC film to allow measurement of absolute dose during the experiment. The experiment also included characterization of the beam lateral spread. Furthermore, we conducted a theoretical study of the RC film dose response as a function of the linear energy transfer of protons, concluding that RC films show a dose under response in the proximity of Bragg peak (quenching effect). This theoretical study was verified with the measured beam profiles and a Monte Carlo simulation using TOPAS.

2. FOREWORD

FLASH radiotherapy is an emerging radiotherapy technique whose potential as a future treatment against cancer is being investigated by several researchers. The Nuclear Physics Group (GFN) of Universidad Complutense de Madrid (UCM) is conducting FLASH protontherapy preclinical experiments, whose purpose is to evaluate biological parameters which describe the response of tumour and healthy cells after FLASH and normal irradiation. These experiments are taking place in the Center for Microanalysis of Materials (CMAM), a research centre located in Universidad Autónoma de Madrid (UAM) which has an electrostatic ion accelerator.

In particular, this work is focused on the experiment I attended, in which different samples were irradiated with 3-MeV protons at conventional and FLASH dose rates. Irradiated samples were classified into three groups: normal living cells, tumor cells and normal cells associated to tumor. In order to irradiate correctly the samples of interest and evaluate the results, an appropriate dosimetry is needed. In the preclinical experiment carried out in CMAM, radiochromic films were used as dosimeters, and this work is focused on this dosimetry process.

In order to extract dose information from RC films, a thorough process must be followed. First, it is necessary to perform a calibration, a relation between the dose delivered by the accelerator and the optical density of the film (when the film is irradiated it gets more or less dark depending on the delivered dose). Doses delivered during calibration were estimated from known beam intensity and shutter opening times, convoluted with known beam sizes, energy and stopping power at irradiation position. Once calibration curve is calculated, absorbed dose by the samples can be extracted from the radiochromic films darkening.

On the other hand, radiochromic films were also employed in the experiment to carry out measurements of the beam profile. This is used to characterize in-air spread of the beam (which ultimately depends to the beam optics configuration) and it is used by the treatment planning system to calculate adequate shutter times in order to deliver the required doses, taking into account the air distance traveled by the beam before hitting the target.

3. FLASH RADIOTHERAPY

3.1 INTRODUCTION

Nowadays, radiotherapy is one of the main treatments against cancer. Its aim consists in eradicating tumors while protecting as much as possible the surrounding normal tissues. Throughout the years, clinical radiotherapy treatments have experimented different improvements in order to achieve this objective. For example, treatments have been fractionated so that patients are exposed to 1.8-2 Gy per session instead of receiving the total dose in a single session, this way side effects in healthy tissues are reduced. Furthermore, technology development has allowed optimizing the irradiated volume, reducing the body region which is going to be exposed to radiation.

In the recent years, a different factor is being taken into account in order to protect normal tissues, irradiations with ultra high dose rates. This way, total dose can be delivered in ms and, consequently, treatment duration is notably shortened. This modality is named FLASH radiotherapy, an emerging technique which employs dose rates 100 times higher (> 40 Gy/s) than the ones utilized in conventional radiotherapy ($\leq$0.03 Gy/s). FLASH radiotherapy potential is currently being investigated and, although further research is needed, different preclinical experiments, employing FLASH irradiation, have shown a protective effect in healthy tissues while maintaining the antitumor efficiency. This reduction of normal tissues damage is named FLASH effect.

The biological reasons why the protective effect is observed have been investigated by several researchers, and different hypothesis have been proposed. Some of the theories are based on the fact that tissues with low oxygen concentration are more resistant to radiation than well oxygenated tissues (Pratx, 2019) (Montay-Gruel, 2019). A particular study consisted in investigating the impact of FLASH and conventional irradiation in mice memory as a function of oxygen concentration in the brain and free radicals production (Montay-Gruel, 2019). It was hypothesized that ultra high dose rate irradiation reduce the production of free radicals through a fast depletion of oxygen concentration (high concentration of free radicals cause damage in DNA, cellular structures, etc, it favors carcinogenesis). To test this theory, brain oxygen concentration in mice was doubled (breathing carbogen), and it was shown that the increase in oxygen concentration implied the loss of the neurocognitive benefits previously observed with FLASH irradiation. Furthermore, the production of H_2O_2 (a type of toxic free radical resulted from radiolysis) was measured and a notably lower concentration of H_2O_2 with FLASH irradiation compared to conventional irradiation was obtained. It can be concluded as a possible biological explanation that FLASH radiotherapy benefits depend on local oxygen concentration and free radicals production.

3.2 CURRENT EVIDENCE FOR FLASH RADIOTHERAPY

While the first works on high dose-rate effects in radiotherapy date back from more than four decades ago (Dewey, 1969), this effect was re-discovered in 2014 (Fauvadon, 2014) and has since then gained enormous momentum. A number of in-vitro and in-vivo preclinical studies have been reported and finally, in early 2019, the first patient was treated in a Swiss hospital (Bourhis, 2019).

In this section, seven preclinical experiments and a clinical treatment are described. Six of them are in-vivo preclinical trials, while only one reports findings based on in-vitro cell cultures. More than 70% of the analyzed experiments support the advantages of FLASH radiotherapy versus standard-rate radiotherapy.

3.2.1 IN-VIVO PRECLINICAL STUDIES

Fauvadon et al (Fauvadon, 2014) performed the first in-vivo experiment to explore the potential of ultra-high dose rate irradiation in radiotherapy. In order to evaluate the potential of FLASH, it was analyzed the effect of FLASH and conventional-rate electrons in terms of tumor control and related complications, such us, development of pulmonary fibrosis and the occurrence of apoptosis (a form of cell death) in mice.

Related to the study of lung fibrosis, mice were irradiated with 17 Gy at FLASH (60 Gy/s) and conventional (0.03 Gy/s) dose-rates, as well as with 30 Gy in FLASH mode. The results reported that mice exposed to 17 Gy-CONV showed initial signs of fibrosis 8 weeks post-irradiation, and 24 weeks later massive fibrotic lesions were observed. In the 17 Gy-FLASH-group fibrosis was not observed, and 24 weeks after, only a few of the mice exposed to 30 Gy-FLASH developed fibrotic patches. FLASH radiotherapy seemed to be less fibrogenic than conventional radiotherapy. Additionally, tumor growth was followed by bioluminescence analysis (Fig 1).

Tumor growth in the control group was fast and, as a consequence, individuals had to be euthanized. There were two 15-Gy-CONV survivors cured, but they presented fibrotic remodeling. In contrast, there were seven 28-Gy-FLASH survivors, most of them tumor-free, and they did not present initiation of fibrosis.

Overall, their results determined that FLASH improved the differential response between normal tissue and tumor, preventing side effects and controlling the tumor. This experiment had a high relevance and motivated more researchers to investigate further into the FLASH effect.

The protective effect of FLASH on normal tissues, specifically on brain tissues, was studied in different occasions in the recent years. In 2017, the preservation of memory and neurogenesis (birth of new neurons) in mice hippocampus after whole brain irradiation, using

electron beams, was investigated (Montay-Gruel, 2017). And it was concluded that damage to normal-brain tissue could be reduced by increasing the dose rate. One year later, another in-vivo experiment was designed to assess whether the previous results could be reproduced with X rays generated by a synchrotron (Montay-Gruel, 2018). And protection of normal tissue with FLASH irradiation was also observed.

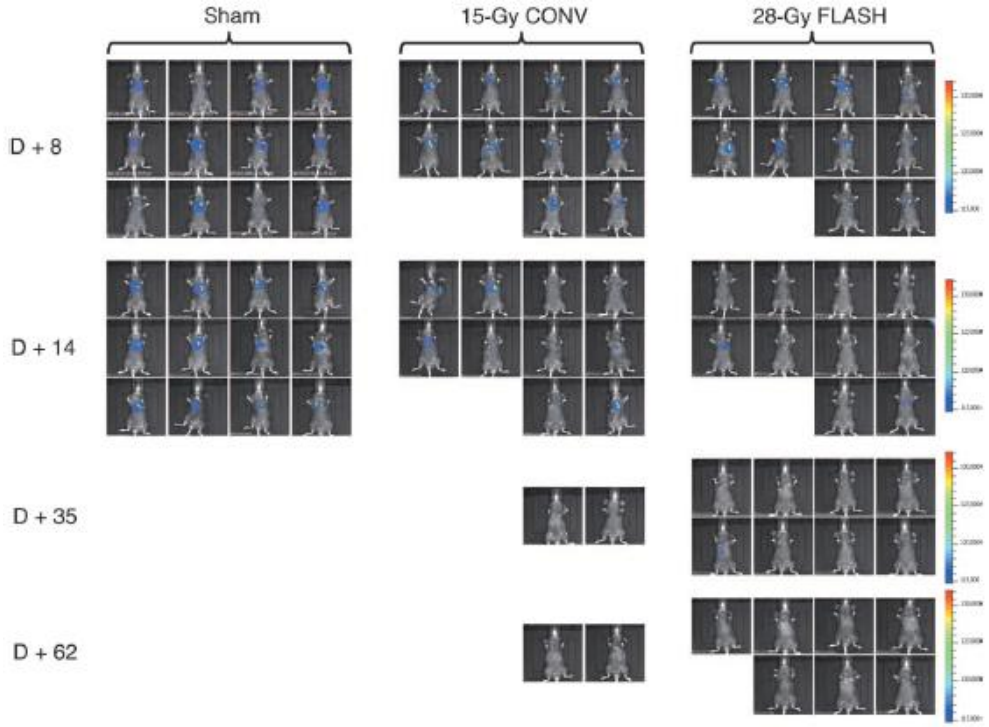

Fig 1. Lung tumor evolution in three different groups: control (0 Gy), mice exposed to 15 Gy at conventional dose rate, and mice exposed to 28 Gy at FLASH rate. Tumor cells were implanted on day D, and two days later mice were treated (Fauvadon, 2014).

Furthermore, in 2019, studies in mice were extended to demonstrate efficacy of FLASH radiotherapy in mini-pig and cat patients (Vozenin, 2019). Two prototypes of linear accelerators, for producing electron beams, were designed. The aim of the study was to evaluate if the differential effect between tumor and normal tissue could also be observed in higher mammals.

In first place, skin patches on the back of the pig (Fig 2) were irradiated with doses ranging from 22 to 34 Gy at standard and FLASH dose rates. 32 weeks after delivering 28-34 Gy at conventional dose rate, depilation and fibrosis was observed. While, after the same time post irradiation (32 weeks) and the same delivered dose (28-34 Gy), at FLASH dose rates, not only fibrosis was not observed but also hair was regrowing. These results confirmed that FLASH-RT is a non-fibrosing modality (it does not produce the formation of excess fibrous tissue in an organ or tissue in a reparative process) compared to conventional-RT. It motivated the researchers to perform a dose-escalation FLASH-RT clinical trial where six cats with

squamous-cell carcinoma of the nasal planum were treated with radiotherapy in a single fraction.

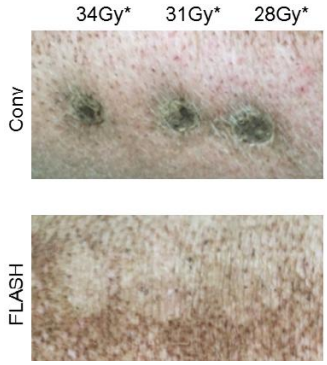

Fig 2. Skin patches on the back of the pig 36 weeks after being irradiated at conventional and FLASH mode (Vozenin, 2018).

Their results reported a remarkable normal tissue tolerance to the high single dose and a high tumor control rate (Fig 3). Five out of six cats experienced the disappearance of all clinical evidence of tumor. This study is an important contribution for the possible translation of FLASH radiotherapy to clinical practice.

Fig 3. Evolution of the lesion in cat n°2 over time. A- Before radiotherapy, B- 7 months post FLASH radiotherapy, C- 14 months post FLASH radiotherapy (Vozenin, 2019).

Up to now, in-vivo experiments which demonstrate FLASH effect generated by photon and electron beams have been mentioned. But, in recent years, researchers have also made studies related to proton FLASH irradiation.

In 2019 the first in-vivo study of the proton FLASH effect was published (Beyreuther, 2019). However, the results did not show the expected protective effect on normal tissue.

In the experiment Zebrafish embryos were irradiated at conventional (5 Gy/min) and FLASH (100 Gy/s) dose rate with a proton beam. To evaluate the potential of proton FLASH therapy, embryonic survival, pericardial edema as acute radiation effect and parameters indicators of morphological malformations were analyzed. The results concluded that there was no difference in the response of embryonic survival and malformations between the embryos irradiated at FLASH and conventional dose rates. The only result that supported the FLASH protective effect was the rate of pericardial edema, which was lower when dose was delivered at FLASH dose rates compared to conventional dose rates.

3.2.2 IN-VITRO PRECLINICAL STUDIES

In 2019, an in-vitro experiment was published (Buonano, 2019). In it a FLASH dose rate proton machine was used to irradiate normal human lung fibroblasts. The aim of the study was to analyze acute and long term irradiation induced effects in normal cells.

On one hand, positive results respecting FLASH protective effect were obtained. It was observed that ultra-high dose rates improved inflammatory markers responses. But, on the other hand, the results of the evaluation of DNA damage and normal cell survival as a function of dose rate, did not supported the FLASH protective effect. Irradiating cells at higher dose rates did not reduce DNA damage, and it did not increased normal cell survival.

Both proton therapy studies, in vivo (Beyreuther, 2019) and in vitro (Buonano, 2019) obtained contradictory information about FLASH protective effect on normal tissue.

3.2.3 FIRST PATIENT TREATED WITH FLASH RADIOTHERAPY

Positive results of most of preclinical experiments were the base to consider FLASH radiotherapy as a promising option for a patient with cutaneous lymphoma. This patient was 75 years old, and his illness had been treated with nine different treatments over 18 years. As none of them was able to control the disease, it was disseminated throughout the skin surface (Fig 4).

Fig 4. Tumor sites over the skin of the patient (Bourhis, 2019).

Due to the good differential response between normal tissue and tumor offered by FLASH therapy, it was considered as a good option to treat one of the most resistant lesions of the patient. The first treatment of a human with FLASH radiotherapy was carried out in 2019 (Bourhis, 2019). The device used to deliver an electron beam in FLASH modality was a linac prototype, Oriatron eRT6 5.6-MeV.

The dose prescribed for the treatment was 15 Gy given in 90 ms. This decision was taken by the researches after studying the results obtained in previous pre-clinical experiments, such as (Vozenin, 2019). To ensure 15 Gy was exactly the dose delivered on the lesion, dose profiles were measured with GafChromic films before and after the irradiation.

The results showed that tumor started to diminish 10 days post irradiation, a rapid response, and it was completely eradicated at 36 days. On the other hand, skin reactions appeared, but

they were minor reactions compared to previous ones after exposure to prior treatments. In conclusion, positive results regarding tumor control and normal tissue were obtained.

This first patient treatment demonstrated the feasibility of FLASH radiotherapy for clinical application.

3.3 DOSIMETRY

In every radiotherapy treatment or irradiation one of the main parts of the process is the dosimetry. Prior to any irradiation it is really important to make dose measures and check that the dose which is going to be delivered follows the planned conditions. For example, checking that the correct amount of Grays is delivered and which regions of the patient body or sample are going to be exposed to that dose. Dosimeters are the instruments employed to conduct these dose measures.

As it was explained in the foreword of this work, Nuclear Physics Group (GFN) carried out a preclinical FLASH protontherapy experiment at CMAM facility. The aim of the experiment was to investigate the potential of FLASH protontherapy comparing the different samples response after FLASH and conventional irradiation. The dosimeters employed in this study were radiochromic films, and in the next sections it is going to be explained the whole dosimetry process.

4. RADIOCHROMIC FILMS FOR PROTON DOSIMETRY

Radiochromic films are chemical passive dosimeters. When these films are irradiated chemical reactions are induced, in particular, polymerization reactions. RC films material is presented as monomers, when dose is delivered these monomers are joined forming polymers (longer chains) and, consequently, film optic properties are altered. This process is due to the activity of free radicals generated by radiation. In particular, the materials which produce the coloration of the film are crystalline polyacetylenes (Das, 2017, 373), when they are exposed to radiation polymerization takes place and film darkening is visualized. The higher the dose delivered is, the darker the film gets. This way, the absorbed dose by the film can be known from the variation of its optical density (OD).

4.1 CURRENT STATE OF THE ART

Radiochromic films have been employed as radiation dosimeters since 1960, although not for clinical use. In mid-1980s, the radiochromic film known as GAFchromic was produced by the International Specialty Products (ISP) (Das, 2017, 373). Several radiochromic film types have been developed by different manufacturers along the years, so this section is going to focus on the available GAFchromic RCF products which have useful dose ranges for clinical radiotherapy applications.

In 2004, EBT film was introduced, a more sensitive radiochromic film model than previous ones. Five years later, EBT films were replaced by EBT2 films which have the same active component as the EBT but it has a single active layer (the sensitive material to radiation). EBT2 films have a type 2 configuration shown in Fig 5. In order to eradicate the dependence on which side of the film faces the light source of a scanner or the radiation source, EBT3 films were introduced. In both EBT2 and EBT3 films, the active layer is protected by two polyester layers, however EBT3 have a symmetric configuration (type 3 configuration in Fig 5).

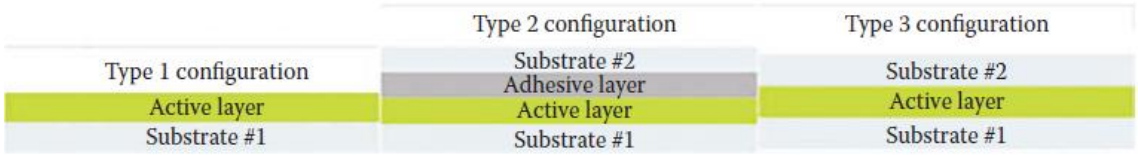

Fig 5. Radiochromic film type 1, type 2 and type 3 configurations (Das, 2017, 373).

The most interesting radiochromic film configuration for this work is type 1, unlaminated EBT3 films. These films were the ones utilized in the CMAM experiment whose dosimetry is made in next sections. As the beam energy of the experiment was low (3 MeV), protons range in material is short and would otherwise be stopped in the film substrate, not reaching the active layer. So we employed unlaminated EBT3, a EBT3 model in which the upper polyester layer has been removed.

The use of radiochromic films as reference dosimeters for radiotherapy or preclinical experiments provides some advantages and disadvantages. These films offer a near-tissue equivalence and a submillimetric spatial resolution, however, RC films can be damage if they are exposed to high temperatures (>60ºC) or to room light.

Scientists have experimentally studied RC films suitability for complex radiotherapy dosimetry in the recent years. In particular, interesting results for low energy protons were obtained in an experiment conducted in 2015 (Reinhardt, 2015). Dose response curves of EBT2 and EBT3 films for 20 MeV protons and 6 MeV photons were compared and no significant difference was observed. However, an under response was visualized in the 4 MeV protons dose response curve, in the proximity of the Bragg peak. This low-energy effect with protons (quenching effect) will be studied in the section 4.3.2. If this effect is taken into account RC films can be used as reference dosimeters for low energy proton measures. Furthermore, in 2017, it was demonstrated that EBT3 films response is energy and mean dose-rate independent (Jaccard, 2017). In that investigation a clinical radiotherapy linac (Eleka Synergy) and a prototype high dose-rate linac (Oriatron eRT6) were employed to deliver electron beams. EBT3 films suitability for high dose-rate measurements was confirmed.

4.2 METHODOLOGY

In the experiment performed at CMAM, radiochromic films were employed as dosimeters for FLASH protontherapy. The aim of its use was to verify that the dose absorbed by the irradiated sample and the planned dose corresponded. The films employed were unlaminated EBT3 (lot 11181901P1).

Films were placed at the end of the beam and perpendicular to the direction of the beam axis, in the same conditions in which samples would be irradiated later. As unlaminated EBT3 films have an asymmetric configuration, care was taken ensuring that the same film side was facing the beam exit. Films were irradiated with a 3 MeV proton beam. Subsequently, they were scanned. It is important to wait at least 12 hours between exposure and digitalization because of the change of the optical density, films continue getting darker after exposure. In particular, the ones used for calibration were scanned 12 hours after irradiation. The scanner (HP Scanjet G3110) was employed in transmission mode. Each film was cut into three pieces before scanning because of the scan window dimensions.

Another aspect to take into account is the position and the orientation of the film on the scanner. The scanner response changes depending on how near to the scanner axis the film is (Micke, 2011), lateral artifact effects are minimized if the film is positioned along the central axis and parallel to the scan direction. Furthermore, all films were scanned positioning the most sensitive side of the film on the scanner.

4.3 RESULTS

4.3.1 PREPARATION OF RADIOCHROMIC FILMS

4.3.1.1 RADIOCHROMIC FILM CALIBRATION

In order to obtain the dose delivered to the film, a calibration curve is needed, a relation between dose and optical density, OD, (film darkening). Although higher levels of dose induce higher values of OD, this relation is not usually linear. Several calibration curves have been utilized by the authors of different studies conducted in the recent years.

The method which is going to be employed to evaluate radiochromic film dosimetry is a multichannel film dosimetry method. The scanner used for digitizing films is a multichannel one, it consists of three channels: red (R), blue (B) and green (G)). Optical density obtained from the three different channels will allow distinguishing between the part of the film response that depends on the dose delivered and the part of the film response that is dose independent. This second part will inform about film imperfections like active layer thickness variations.

First of all, calibration films were irradiated with a plan that delivers twelve radiation pulses in a dose range from 1 Gy to 12 Gy, Fig 6.

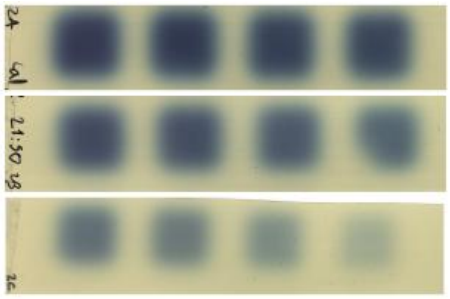

Fig 6. Radiochromic film employed for calibration.

Where 65535 is the maximum pixel value (16-bit TIF format was used), and each channel provides a different value of OD (as it is observed in Fig 7). Subsequently, calibration curve can be obtained, dose (D) and OD are fitted according Eq.1 from Micke et al. 2011. It is represented in Fig 7.

$$\mathrm{OD} = -log\left(\frac{a+b\cdot D}{c+D}\right) \quad (1)$$

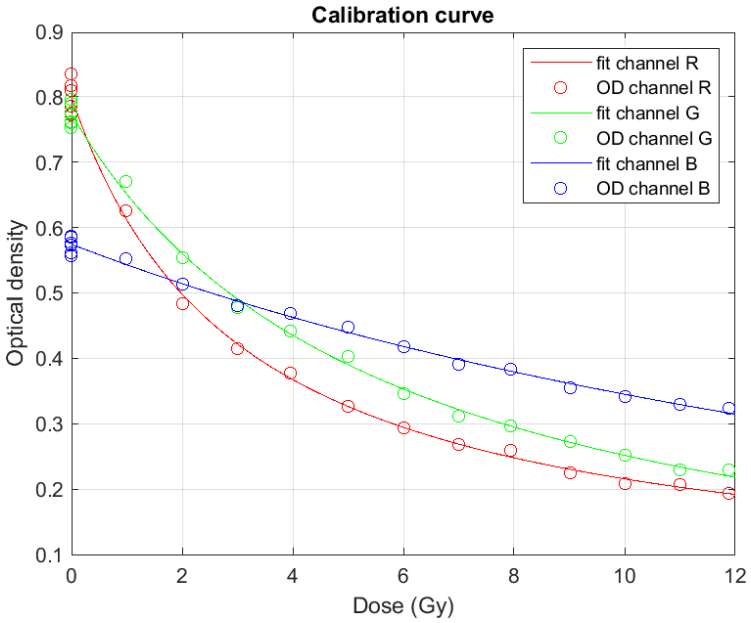

Fig 7. Multiple channel calibration curves.

It must be pointed out that calibration curves perfectly agree with each channel OD values. Fit parameters are given in Table 1.

Table 1. Calibration curve parameters (Eq.1) for each channel.

Channel	a	b	c
R	2.44539	0.03703	3.05876
G	4.38756	-0.04446	5.67209
B	13.55192	-0.19617	23.59271

4.3.1.2 LEAST SQUARES METHOD FOR DOSE CALCULATION

As a triple-channel film dosimetry method is being used, the scanned optical density can be separated in two different parts, the dose dependent one and the optical density on account of disturbances such as variation of the film active layer thickness. If these two parts are not distinguished, film imperfections could lead to erroneous dose values.

The dose value given by each channel can be calculated following Eq.2. Where Eq.2 has been estimated solving the dose, D, from Eq.1, and including the disturbance, active layer thickness variations, in the optical density term (multiplying OD·Δd). Δd is defined as $\Delta d = \frac{\tau}{\bar{\tau}}$ where τ is the active layer thickness and $\bar{\tau}$ the average film thickness.

$$D = \frac{10^{-OD \cdot \Delta d} \cdot c - a}{b - 10^{-OD \cdot \Delta d}} \quad (2)$$

Each channel provides different dose values, D_R, D_G and D_B. The difference between these dose values, Ω, is minimized employing a least square equation, Eq.3. Ω has to be minimized because the dose can not depend on the chosen channel.

$$\Omega = (D_R - D_G)^2 + (D_R - D_B)^2 + (D_B - D_G)^2 \quad (3)$$

The values of the disturbance parameter, Δd, were chosen in the range from 0.8 to 1.2. Final value was selected so that is minimum, $\frac{d(\Omega)}{d(\Delta d)} = 0$. Δd values corresponding to the minimum Ω value for each pixel will determine the dose independent part of the film response (disturbance map). Therefore, D_R, D_G and D_B are calculated for these disturbance values following Eq.2. Subsequently, the final measured dose is obtained as the average of D_R, D_G and D_B, Eq.4.

$$D_{measured} = \frac{D_R + D_G + D_B}{3} \quad (4)$$

Figure 8 (left side) shows the scanned image of an unlaminated EBT3 film exposed to 2 Gy. That figure (right side) also shows the simulation of the radiochromic film, how the non irradiated film would look like if it did not have any imperfection. Furthermore, the dose map, whose dose values have been calculated using Eq.4, and the disturbance map are represented in Fig 9. The scanned film shows some inhomogeneities like dust particles in the centre of the image. These imperfections are also observed in the disturbance map, however, the dose map is homogeneous. Triple-channel method has separated the dose independent part of the film response (disturbance map), from the dose dependent part (dose map).

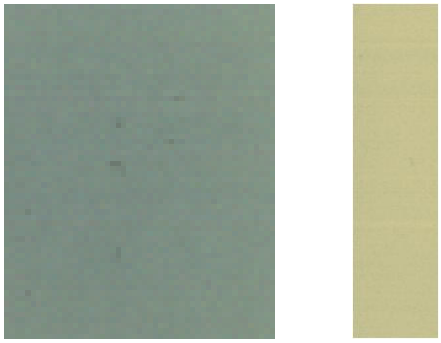

Fig 8. EBT3 film exposed to 2 Gy (left image) and the non irradiated radiochromic film (right image).

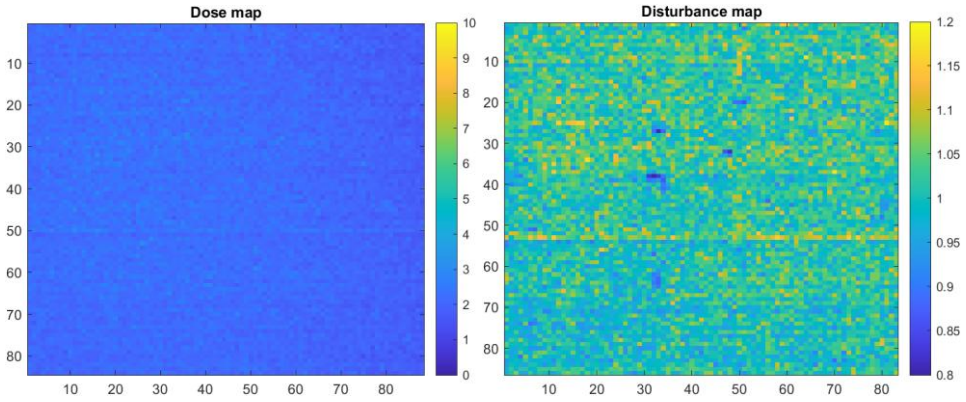

Fig 9. Dose map and disturbance map for the scanned film shown in Fig 8.

4.3.2 QUENCHING THEORETICAL STUDY

Radiochromic films response in different conditions has been investigated by several researchers. From the different experiments, the energy independence of films response was confirmed with an exception, films exposed to low energy proton beams. In that case, radiation induced optical density values lower than it should be in the proximity of the Bragg peak. This film under-response is named quenching effect.

There are two hypothesis to explain quenching effect (Grilj, 2018). On one hand, in the film crystal lattice, polymerization sites are spaced with some separation. High LET radiation could activate the polymerization of all sites in the neighborhood of a single ionizing particle track. This way, there is a moment in which all polymerization sites are activated and the film is saturated. In that conditions although the film is exposed to additional radiation it is not going to induced more polymerization or film darkening, so dose values extracted from the optical density will be lower than the real dose absorbed by the film. On the other hand, it exists the possibility that high-LET radiation generates fewer polymerization than low-LET radiation. The reason would be that high LET particles could lead to the formation of a higher density of free radicals and, consequently, they could recombine without initiating polymerization. Fewer polymerization imply fewer film darkening.

The aim of this section is to show quenching effect employing LET values obtained from NIST website and calculations developed in a Matlab program. If initial particles energy (3 MeV) and travelled distance (20 cm) are introduced, then the Matlab code obtains particles in-water stopping power of particles at the position of the RC film. This way, 3 MeV protons employed in CMAM experiment were simulated. In order to quantify the dose under-response or quenching effect, we employed the relative efficiency (RE) parameter. Researchers have utilized similar RE definitions, for example Reinhardt et al (Reinhardt, 2015) define it as the range of dose values that, deriving from different beam energies, lead to the same film response. Each researcher utilizes a different relation between LET and RE, as Reinhardt et al used 4 MeV protons in their study its RE expression, equation (5), was used to calculate RE values corresponding to our 3 MeV protons.

$$RE = 100\% - a \cdot LET \cdot b \tag{5}$$

Where a and b are fit parameters. However, this expression was not suitable for our 3 MeV protons, LET values were so high that negative RE values were obtained. We needed a RE expression appropriate for high LET particles. In 2018, a study was published in which RC films response was investigated with MeV ions beams (Grilj, 2018) and a modified RE expression was shown, equation (6). In this equation the LET dependence of the film response was introduced in the parameter $D_{1/2}$, which is the dose corresponding to one half of the maximum optical density (maximum film darkening).

$$RE = \frac{D_{\frac{1}{2}}(0)}{D_{\frac{1}{2}}(LET)} = \frac{D_{\frac{1}{2}}(0)}{a \cdot LET + D_{\frac{1}{2}}(0)} \tag{6}$$

$D_{1/2}(0)$ represents the infinitesimally small LET value. It can be considered as the $D_{1/2}$ corresponding to low LET radiation, for example, photon beams. Due to the proximity between the data utilized in this study (low energy protons and ions, and high LET range) and the data employed in our simulation, the parameter $D_{1/2}(0)$ = 45 Gy was taken from Grilj et al study. In order to obtain the slope 'a' of the linear relation between $D_{1/2}$ and LET and its uncertainty, the bootstrapping method was applied. The practice of bootstrapping basically consists in estimating the uncertainty of a parameter (a) from two variables with its respective uncertainties (LET and $D_{1/2}$). Employing LET and $D_{1/2}$ values provided in the study, with Matlab help, we generated random points inside the Gaussian distributions centered at LET_i and $D_{1/2_i}$ with standard deviations ΔLET_i and $\Delta D_{1/2_i}$. This way each coordinate (LET, $D_{1/2}$) was calculated several times and in each iteration a linear regression was made, obtaining the slope 'a' 10^4 times. This way the mean and the standard deviation of all 'a' values resulted in $a \pm \Delta a = (0.4960 \pm 0.0576) \frac{\mu m}{keV}$.

Introducing LET values in equation (6) the relative efficiency was calculated and, consequently, quenching effect can be evaluated. Fig 10 shows how RE decreases when LET increases. Meaning that the higher the LET, the higher the difference between the dose delivered to the film and the dose measured from the film: quenching effect increases with LET. In addition, Fig 11 clearly shows that this effect takes place in the proximity of Bragg peak. If both graphics in Fig 11 are compared, a notable decrease in RE is observed at the distance where Bragg peak is.

On the whole, quenching effect has been theoretically demonstrated and, as a consequence, it can be concluded that RC films response has a high dependence on the beam exit – RC film distance. In Fig 11 it can be seen that RC film is less efficient when the distance increases, so this effect has to be taken into account when RC films are employed as dosimeters for irradiation with high LET particles.

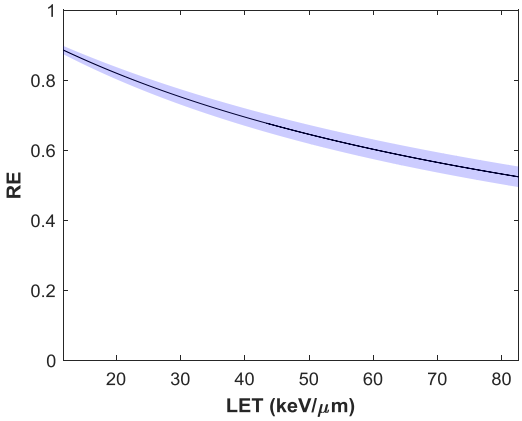

Fig 10. Relative efficiency as a function of LET. RE error was calculated as a consequence of parameter 'a' uncertainty (blue bands). Relative errors are less than 6%.

4.3.3 DOSIMETRY FOR SAMPLE IRRADIATION

In the CMAM experiment different samples were irradiated, in particular breast cancer cells and fibroblasts. Cells were contained in wells and plates, with circular and rectangular shape respectively. The aim of samples irradiation was to deliver the same dose with FLASH dose rates and with conventional dose rates, and observing cells response after both irradiation modes. In order to check the dose delivered to the cells in each mode, radiochromic films were employed. Unlaminated EBT3 films were exposed to the same irradiation plans as samples.

In the case of well dosimetry, results are shown in table 2, where dose measures have been obtained for circular regions with well radius. If doses obtained with FLASH and conventional irradiation are compared, it can be seen that both groups of values are similar with the exception of the two highest doses delivered (shots 5 and 6), whose values differ in 1 and 2 Gy from FLASH to conventional mode.

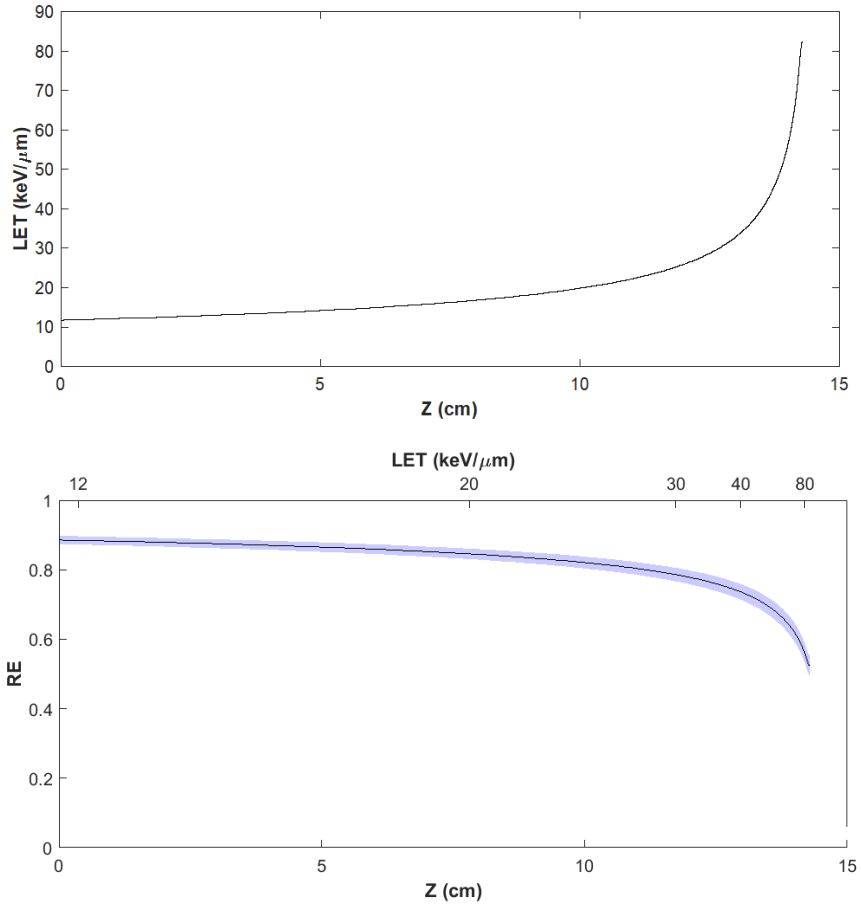

Fig 11. Water Bragg peak for 3 MeV protons (up), and the relative efficiency as a function of LET and traveled distance (down). RE error was calculated as a consequence of parameter 'a' uncertainty (blue bands).

Table 2. Dose measured from RC films utilized for wells dosimetry.

	FLASH		**CONVENTIONAL**	
Shot number	**D (Gy)**	**ΔD (Gy)**	**D (Gy)**	**ΔD (Gy)**
1	1.3987	0.0278	1.1497	0.0077
2	1.8706	0.0697	1.999	0.0716
3	3.7009	0.1439	3.1946	0.0934
4	5.4932	0.3644	5.9219	0.0818
5	11.1675	0.3708	10.5119	0.3685
6	16.5965	0.5106	14.5874	0.2856

Furthermore, results obtained for cells contained in plates are shown in Fig 12 (after FLASH irradiation) and Fig 13 (after conventional irradiation). In them, dose distribution and dose histograms for each irradiated region of the RC film are shown. These dose measures have been calculated for rectangular regions with plate dimensions. The fact that the scanned RC film might be rotated a certain angle with respect to the horizontal scanner axis has also been taken into account.

If figures 12 and 13 are compared, it can be seen that dose delivered with FLASH and conventional dose rates is not the same. The unlaminated EBT3 film exposed to FLASH irradiation received higher dose values than the one exposed to conventional dose rates, probably due to fluctuations in beam current or an incorrect estimation of beam size and shape at the irradiation position.

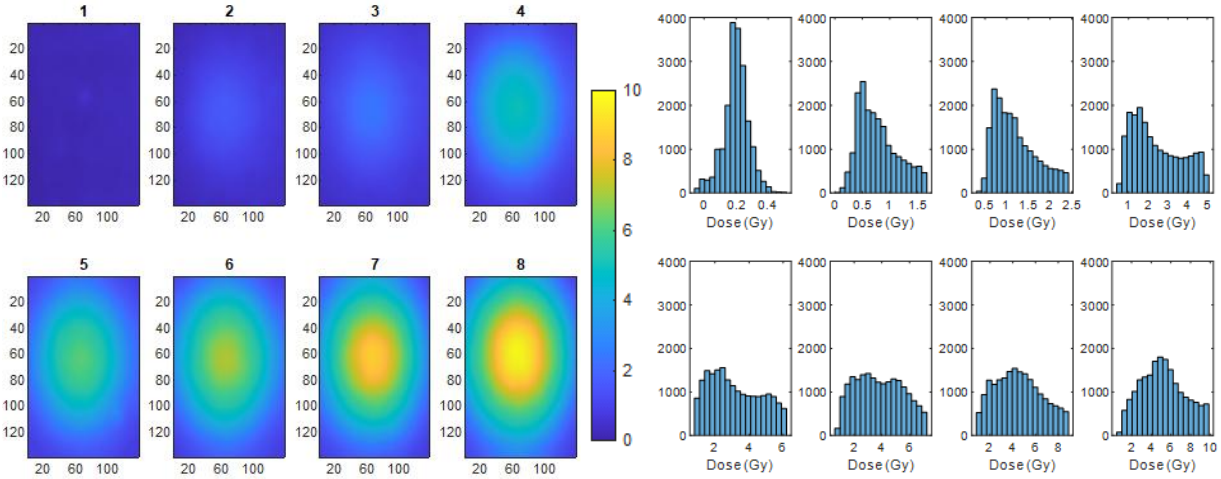

Fig 12. FLASH irradiation results. Dose maps for each spot (left side) where the color bar indicates a dose range from 0 to 10 Gy. In the right side its corresponding dose histograms are shown.

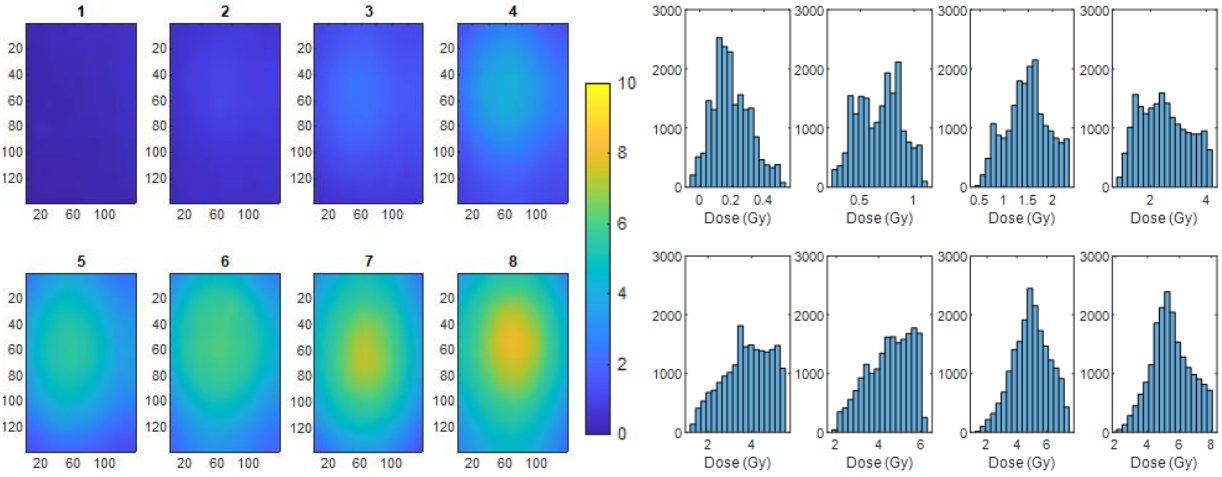

Fig 13. Conventional irradiation results. Dose maps for each spot (left side) where the color bar indicates a dose range from 0 to 10 Gy. In the right side its corresponding dose histograms are shown.

4.3.4 BEAM PROFILE MEASURES IN AIR AND QUENCHING VERIFICATION

Unlaminated EBT3 films were also utilized for beam profile measurements. These were conducted with and without pepperpot, a pinhole filter used to reduce the beam intensity for certain experiments. Measurement process consisted in irradiating different spots of the film while the distance between the film and the beam exit increased. Initial film-beam exit distance was 4.9 cm and it increased 1.5 cm between each spot irradiation. This process was repeated twice for each film, delivering low and high dose on the RC film spots. In the second

part of the irradiating process the number of FLASH shots delivered in each spot of the film was higher. The visual result of the whole irradiating plan is shown in Fig 14.

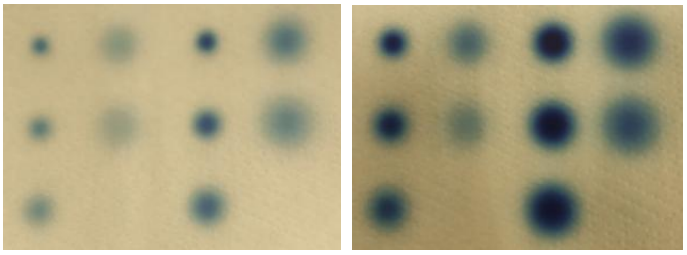

Fig 14. Unlaminated EBT3 film exposed to the measuring beam profile irradiation plan. In the left image pepperpot was not employed, while in the right image it was used.

In the case in which pepperpot is not used, in the first part of the irradiating process (columns 1 and 2 of Fig 14 (left side)) 2 FLASH shots were delivered in each film spot, and in the second part (columns 3 and 4) higher dose was utilized, 6 FLASH shots in each spot. The duration of each shot duration was 0.75 ms. Furthermore, when irradiation was carried out with pepperpot (Fig 14 (right side)), low dose spots where exposed to radiation during 50 ms and high dose spots during 250 ms.

The followed process to obtain the profile measurements was the same for both irradiation modes (with and without pepperpot). Unlaminated EBT3 films were exposed to high doses (D_{high}) and low doses (D_{low}), where $\frac{D_{high}}{D_{low}} = x$. The objective is to employ the information provided by both spot types (high and low doses) to measure the dose central value and the beam width (σ) as a function of the distance. Considering that high dose spots saturate (its darkening is maximum) at the centre of the region, they will just provide correct information about the periphery of the spots. However, low dose spots will inform correctly about the central region. This is the reason why the best option is to integrate both spots types information. In order to integrate that information, low doses are multiplied by the factor x so that high and low doses are equalized. Then, for each pixel, the maximum value between D_{high} and $x \cdot D_{low}$ is chosen and employed in the final dose distribution. From this final dose distribution σ_x and σ_y are obtained (beam width in x and y axis).

The dose value in the central point of each spot and the beam width (σ_x and σ_y) are represented as a function of the air distance traveled (z) in Fig 15. It should be pointed out that the relation between σ and z follows a second grade polynomial (fit parameters are given in Table 3). The longer the traveled distance is, the wider the beam gets and the lower the central dose is. Dose values with pepperpot are higher than without pepperpot due to the fact that when the filter is used, beam intensity is reduced but exposure time is increased.

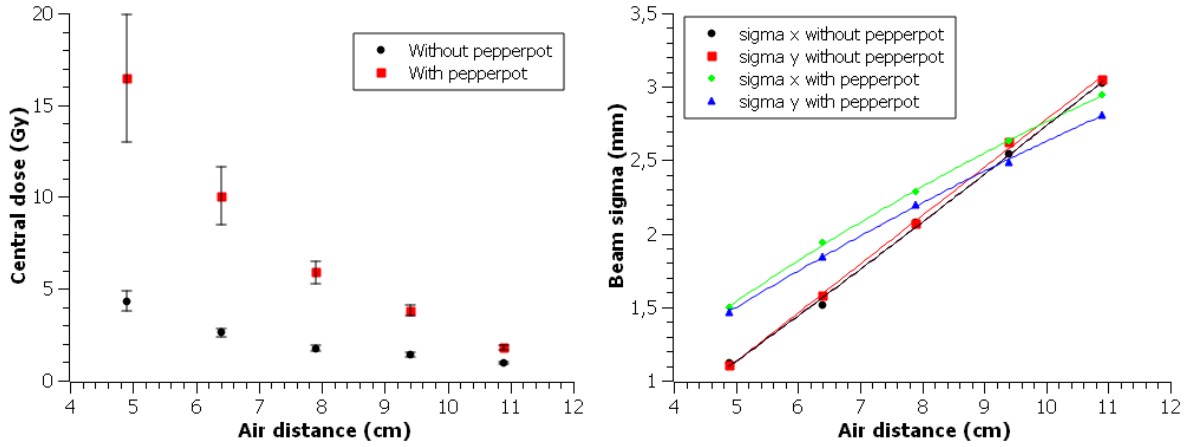

Fig 15. (Left side) Dose at the centre of each spot as a function of the air distance traveled for both irradiation modes, with and without pepperpot. (Right side) Beam width in x and y axis as a function of the air distance traveled. Second grade polynomial fit parameters are shown in table 3.

Table 3. Fit parameters for the second grade polynomial relation between beam width and traveled distance.

		$y = a \cdot x^2 + b \cdot x + c$		
		a	**b**	**c**
Without pepperpot	**sigma x**	0.0024	0.2840	-0.3522
	sigma y	-0.0008	0.3415	-0.5623
With pepperpot	**sigma x**	-0.0080	0.3642	-0.0846
	sigma y	-0.0055	0.3088	0.0896

In order to check if there is an under response (quenching effect) in the dose central measures, experimental dose measures (without pepperpot) were compared with the ones obtained by estimating the average LET with a Monte Carlo simulation in TOPAS and using expression 6 (Grilj, 2018) to determine the expected RE. Fig 16 shows the tendency of both groups of dose values normalized to the first point. In this figure it can be seen that experimental values are lower than simulated ones, there is a dose under response in RC films measures, a quenching effect. Illustrative quenching measures can be given by relative efficacy (RE) calculation, $\mathrm{RE} = \frac{\mathrm{dose_{exp}}}{\mathrm{dose_{MC}}}$. Where normalized RE results are given in table 4.

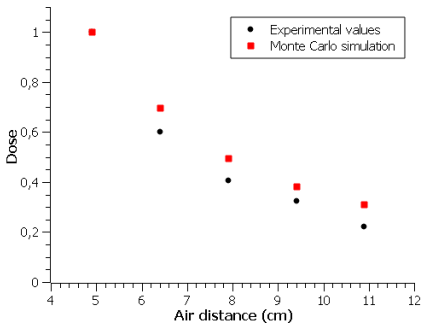

Fig 16. Normalized central dose as a function of the air gap. Where experimental dose values are the ones extracted from RC films.

Table 4. Experimental RE results obtained from measurement.

d (cm)	4.9	6.4	7.9	9.4	10.9
RE (%)	100	86	82	85	72

It can be seen that RE decreases until 72%, showing a notable quenching effect as it was predicted by the theoretical calculation made in section 4.3.2. In order to describe the effect correctly, a thorough study is needed. A whole analysis, including further irradiations, is being prepared and will be published in a peer-reviewed article.

5. CONCLUSION

The dosimetry conducted in this work, employing radiochromic films for monitoring a preclinical FLASH protontherapy experiment, has produced a number of results. On one hand, RC films utilized for measuring the doses received by cellular were slightly different between FLASH and conventional irradiation. Further analysis must be conducted in order to interpret the biological results (toxicity, proliferation) of the experiments.

On the other hand, we conducted a study on the quenching effect on unlaminated EBT3 films for low-energy protons. Application of existing results to our setup predicts that radiochromic films, employed for monitoring 3 MeV protons, are subject to lower relative efficiencies in the proximity of Bragg peak. This effect must be characterized carefully in order to use RC films for absolute dosimetry. This highlights also the importance of knowing with great accuracy the position (i.e. the amount of air) of the samples, relative to the beam exit window. In addition, the quenching effect has been experimentally proved from the conducted beam profile measures. As dose values were obtained as a function of the distance between the film and the beam exit, this group of values was compared with the ones obtained from a Monte Carlo simulation and a dose underestimation was observed in experimental values. The measured RE values follow the same tendency as the (few) values from the literature, but our data suggest that the effect might be larger than has been published so far. This calls for further experiments, which will be soon performed.

On the whole, radiochromic films can be utilized for FLASH and conventional irradiations dosimetry whenever quenching effect is taken into account when high LET particles are employed. Furthermore, after the made bibliographic research about the current state of FLASH radiotherapy, it can be concluded that it is a technique whose potential as a future treatment against cancer is promising. And in order to make possible that the great advantages offered by this radiotherapy technique can be applied to the clinical ambit, further investigation is needed.

6. BIBLIOGRAPHY

Beyreuther, E., Brand, M., Hans, S., Hideghéty, K., Karsch, L., Leßmann, E., ... & Pawelke, J. (2019). Feasibility of proton FLASH effect tested by zebrafish embryo irradiation. *Radiotherapy and Oncology*, *139*, 46-50.

Bourhis, J., Montay-Gruel, P., Jorge, P. G., Bailat, C., Petit, B., Ollivier, J., ... & Germond, J. F. (2019). Clinical translation of FLASH radiotherapy: Why and how?. *Radiotherapy and Oncology*, *139*, 11-17.

Bourhis, J., Sozzi, W. J., Jorge, P. G., Gaide, O., Bailat, C., Duclos, F., ... & Moeckli, R. (2019). Treatment of a first patient with FLASH-radiotherapy. *Radiotherapy and oncology*, *139*, 18-22.

Buonanno, M., Grilj, V., & Brenner, D. J. (2019). Biological effects in normal cells exposed to FLASH dose rate protons. *Radiotherapy and Oncology*, *139*, 51-55.

Das, I. J. (Ed.). (2017). *Radiochromic film: role and applications in radiation dosimetry*. CRC Press.

Dewey, D. L. (1969). An oxygen-dependent X-ray dose-rate effect in Serratia marcescens. *Radiation research*, *38*(3), 467-474.

Favaudon, V., Caplier, L., Monceau, V., Pouzoulet, F., Sayarath, M., Fouillade, C., ... & Hall, J. (2014). Ultrahigh dose-rate FLASH irradiation increases the differential response between normal and tumor tissue in mice. *Science translational medicine*, *6*(245), 245ra93-245ra93.

Grilj, V., & Brenner, D. J. (2018). LET dependent response of GafChromic films investigated with MeV ion beams. *Physics in Medicine & Biology*, *63*(24), 245021.

Jaccard, M., Petersson, K., Buchillier, T., Germond, J. F., Durán, M. T., Vozenin, M. C., ... & Bailat, C. (2017). High dose-per-pulse electron beam dosimetry: Usability and dose-rate independence of EBT3 Gafchromic films. *Medical physics*, *44*(2), 725-735.

Micke, A., Lewis, D. F., & Yu, X. (2011). Multichannel film dosimetry with nonuniformity correction. *Medical physics*, *38*(5), 2523-2534.

Montay-Gruel, P., Acharya, M. M., Petersson, K., Alikhani, L., Yakkala, C., Allen, B. D., ... & Nguyen, T. A. (2019). Long-term neurocognitive benefits of FLASH radiotherapy driven by reduced reactive oxygen species. *Proceedings of the National Academy of Sciences*, *116*(22), 10943-10951.

Montay-Gruel, P., Bouchet, A., Jaccard, M., Patin, D., Serduc, R., Aim, W., ... & Bräuer-Krisch, E. (2018). X-rays can trigger the FLASH effect: Ultra-high dose-rate synchrotron light source prevents normal brain injury after whole brain irradiation in mice. *Radiotherapy and Oncology*, *129*(3), 582-588.

Montay-Gruel, P., Petersson, K., Jaccard, M., Boivin, G., Germond, J. F., Petit, B., ... & Bourhis, J. (2017). Irradiation in a flash: Unique sparing of memory in mice after whole brain irradiation with dose rates above 100 Gy/s. *Radiotherapy and Oncology*, *124*(3), 365-369.

Pratx, G., & Kapp, D. S. (2019). A computational model of radiolytic oxygen depletion during FLASH irradiation and its effect on the oxygen enhancement ratio. *Physics in Medicine & Biology*, *64*(18), 185005.

Reinhardt, S., Würl, M., Greubel, C., Humble, N., Wilkens, J. J., Hillbrand, M., ... & Parodi, K. (2015). Investigation of EBT2 and EBT3 films for proton dosimetry in the 4–20 MeV energy range. *Radiation and environmental biophysics*, *54*(1), 71-79.

Vozenin, M. C., De Fornel, P., Petersson, K., Favaudon, V., Jaccard, M., Germond, J. F., ... & Bouchaab, H. (2019). The advantage of FLASH radiotherapy confirmed in mini-pig and cat-cancer patients. *Clinical Cancer Research*, *25*(1), 35-42.